COO-2318-7

SPECTROSCOPY OF NUCLEAR SYSTEMS

Progress Report

Edward S. Macias

Washington University
St. Louis, Missouri

January 1, 1974 - December 31, 1974

PREPARED FOR THE U. S. ATOMIC ENERGY COMMISSION
UNDER CONTRACT NO. AT(11-1)-2318

DISCLAIMER

Table of Contents

Abstract

The decay of ^{108}Sn, ^{107}Sn, ^{107m}In, ^{106}Sn, ^{97}Pd, ^{96}Pd, ^{140m}Pm, ^{140g}Pm, ^{141}Pm, ^{139}Pr, ^{89m}Nb, ^{89g}Nb, ^{149}Pm, ^{149}Eu and ^{243}Cm have been studied via γ-ray spectroscopy using Ge(Li), Si(Li) and NaI(Tl) detectors. Direct and anti-Compton gamma-ray spectra, γ-γ and x-ray coincidence spectra were employed. A helium jet recoil transport interfaced to a moving tape system was used to study short-lived nuclei.

The energy, spin, parity and lifetimes of levels of ^{93}Mo have been studied via the $^{93}Nb(p,n\gamma)$ and $^{94}Zr(\alpha,2n\gamma)$ reactions using in-beam γ-ray spectroscopy, Doppler shift attenuation, γ-ray angular correlation, and recoil distance methods.

An on-line method for measuring transport time in a helium jet system has been developed. A simple fast sweeping system for extracted cyclotron beams is described. An electron gun for fabricating thin targets and a beta gauge for measuring target thickness are being developed.

High resolution on-line aerosol mass measurement by the beta attenuation technique is described.

Introduction

This work is focused on the study of the nuclear structure of nuclei near closed shells via radioactive decay scheme spectroscopy and in-beam γ-ray spectroscopy. These nearly spherical nuclei are particularly interesting to study because their low-lying levels may be well described by simple nuclear models. In order to have a comprehensive experimental description of these nuclei it is necessary to have lifetimes, spins, and parities of the excited states as well as energies and branching ratios of the γ rays. When possible these quantites are determined by studying γ rays emitted during nuclear reactions as well as γ rays emitting following radioactive decay. In some cases the nucleus of interest can not be studied by simple in-beam reaction spectroscopy because there are no nearby stable nuclei. In these cases the study of short-lived nuclei is one of the best tools for nuclear structure determinations. Part I of this report describes our work in the past year concerning the structure of nuclei near closed shells using decay scheme spectroscopy of short-lived species. Part II of this report describes our recent work on in-beam γ-ray spectroscopy including Doppler-shift lifetime measurements. Part III describes instrument development over the past year and the final section describes the development of a beta attenuation mass monitor for use with atomospheric aerosols. This application of a nuclear technique to an environmental problem was not supported under this contract but is included to indicate another direction of our nuclear chemistry research.

This progress report marks the end of the first 21 months of this AEC contract research. This has been a period of rapid growth and progress in the associated research program. This is the last report in the present

form. Beginning November 1, 1975 this contract, as well as the research conducted by Professors Sarantites and Wahl will be merged with the Washington University Cyclotron operations contract [AT(11-1)-1760].

Publications from the past year

1. "A Simple Fast Sweeping System for Extracted Cyclotron Beams," J.T. Hood, R.A. Goldworm, E.S. Macias, and D.G. Sarantites, Nucl. Inst. and Meth. 119, 213 (1974).
2. "On-Line Determination of Transport Time of a Helium-Jet System," E.S. Macias, R.E. Head, H.-C. Hseuh, and M.R. Zalutsky, Nucl. Inst. and Meth. (in press) (1974).
3. "Anisotropy of Lℓ X Rays and γ Rays in the Decay of ^{243}Cm," M.R. Zalutsky and E.S. Macias, Phys. Rev. (submitted Sept. 1974).
4. "Decay of 5.8-min ^{140m}Pm and 10-sec ^{140g}Pm to Levels of ^{140}Nd," M.R. Zalutsky and E.S. Macias, Phys. Rev. C (submitted October, 1974).
5. "Decay of 40-day ^{103}Ru and 18-day ^{103}Pd to Levels in ^{103}Rh," E.S. Macias, M.E. Phelps, D.G. Sarantites and R.A. Meyer, Phys. Rev. (submitted July, 1974).

Oral Presentations

1. On the Decay of ^{108}Sn, ^{107}Sn, and ^{106}Sn, H.-C. Hseuh and E.S. Macias, American Physical Society Meeting, Washington, D.C., April 23, 1974, Bull. Am. Phys. Soc. 19, 474 (1974).
2. "Lifetimes of Low-Lying Levels of ^{93}Mo via the ^{93}Nb(p,nγ) Reaction," L.L. Rutledge, E.S. Macias and D.G. Sarantites, American Physical Society Meeting, Pittsburgh, Pa., Bull. Am. Phys. Soc. 19, 1003 (1974).

Ph.D. Thesis

"The Application of Nuclear Spectroscopic Techniques to Atomic Systems," Michael Rod Zalutsky, Dec. 1974 (unpublished). Only part of this thesis was supported by the USAEC.

Papers in preparation

1. Structure of N = 81 Nuclei: Levels of ^{141}Nd and ^{139}Ce Populated in Beta Decay," M.R. Zalutsky, E.S. Macias and R.A. Meyer.
2. Lifetime Measurements of Low-lying Levels in ^{93}Mo Populated via the ^{93}Nb(p,nγ) Reaction using the Doppler Shift Attenuation Method," L.L. Rutledge, E.S. Macias, and D.G. Sarantites.
3. Decay of ^{149}Pm and ^{149}Eu to Levels of ^{149}Sm," E.S. Macias and R.A. Meyer.

Papers by the Principal Investigator not supported under this Contract

1. "Angular Correlations between K and L X Rays in the Nd and Tb Atoms," A.L. Catz and E.S. Macias, Phys. Rev. 19, 87 (1974).
2. "K-L X-Ray Angular Correlations in Cm, Pu, and Eu," E.S. Macias and M.R. Zalutsky, Phys. Rev. A9, 2356 (1974).
3. The Angular Correlation of $K\alpha_1$-L X-Ray Cascades in Tantalum, M.R. Zalutsky, E.S. Macias and A.L. Catz, Phys. Rev. (in press).
4. "Experimental Determination of the L_2-L_3X Coster-Kronig Transition Probability in Europium, Plutonium, and Curium," M.R. Zalutsky and E.S. Macias, Phys. Rev. (in press).
5. "Comparison of Techniques for the Determination of the L_2-L_3X Coster-Kronig Transition Probability," M.R. Zalutsky and E.S. Macias, Phys. Rev. (in press).
6. "Measurement of the Angular Correlation between L-M X Ray Cascades," M.R. Zalutsky and E.S. Macias, Phys. Lett. 49A, 285 (1975).
7. "The Angular Correlation of X Rays: L-M Cascades in Plutonium," M.R. Zalutsky and E.S. Macias, Phys. Rev. (submitted October 1974).
8. "High Resolution On-Line Aerosol Mass Measurement by the Beta Attenuation Technique," E.S. Macias and R.B. Husar, Proceedings for the Second International Conference on Nuclear Methods in Environmental Research, edited by J.R. Vogt (in press).

A. Identification of 3-Min ^{107}Sn and 50-Sec 1/2$^-$ Isomer of ^{107}In

This study of the decay of ^{107}Sn is part of our work on the short-lived isotopes near closed nuclear shells. The half life of ^{107}Sn was predicted by Takahasi, Yamada, and Kondoh[1] to be 300 sec and 80 sec for modified Lorentz and Gaussian forms of the single-particle strength function respectively. The beta-decay energy was predicted to be 5.3 MeV by Wapstra and Gove.[2] Systematic analysis of the low-lying levels of odd-A indium isotopes indicates that the first excited state of ^{107}In may be at approximately 700 keV with a spin and parity of 1/2$^-$ and that this state decays via an M4 transition to the 9/2$^+$ ^{107}In ground state.

The ^{107}Sn sources were produced via the ^{106}Cd(^{3}He,2n) reaction (Q = -10.9 MeV) using 95.5% enriched ^{106}CdO targets deposited on 0.01-mm Al foil with spray adhesive. These targets were bombarded with 20-34 MeV ^{3}He ions for 200-400 sec with 2-μA beam intensity. The Washington University helium jet recoil transport interfaced to a moving tape system provided a continuous source of ^{107}Sn activity and minimized the buildup of long-lived products.[3] The singles γ-ray spectrum shown in Fig. 1 was obtained with a 12% true coaxial Ge(Li) detector with energy resolution of 2.2-keV at 1332-keV. The energy and intensity of γ rays with half lives near 3-min are given in Table I. The decay of the intense 678.8-keV γ ray was accumulated in 32 spectra of 25-sec duration each during multiple 400-sec bombardments. The decay curve of this transition shown in Fig. 2 exhibits two components with half lives

---

1. K. Takahasi, M. Yamada, and T. Kondoh, At. and Nucl. Data Tables 12, 101 (1973).

2. A.H. Wapstra and N.B. Gove, Nucl. Data Tables 9, 275 (1971).

3. E.S. Macias, R.E. Head, H.-S. Hseuh, and M.R. Zalutsky, Nucl. Inst. and Meth (1974) (in press).

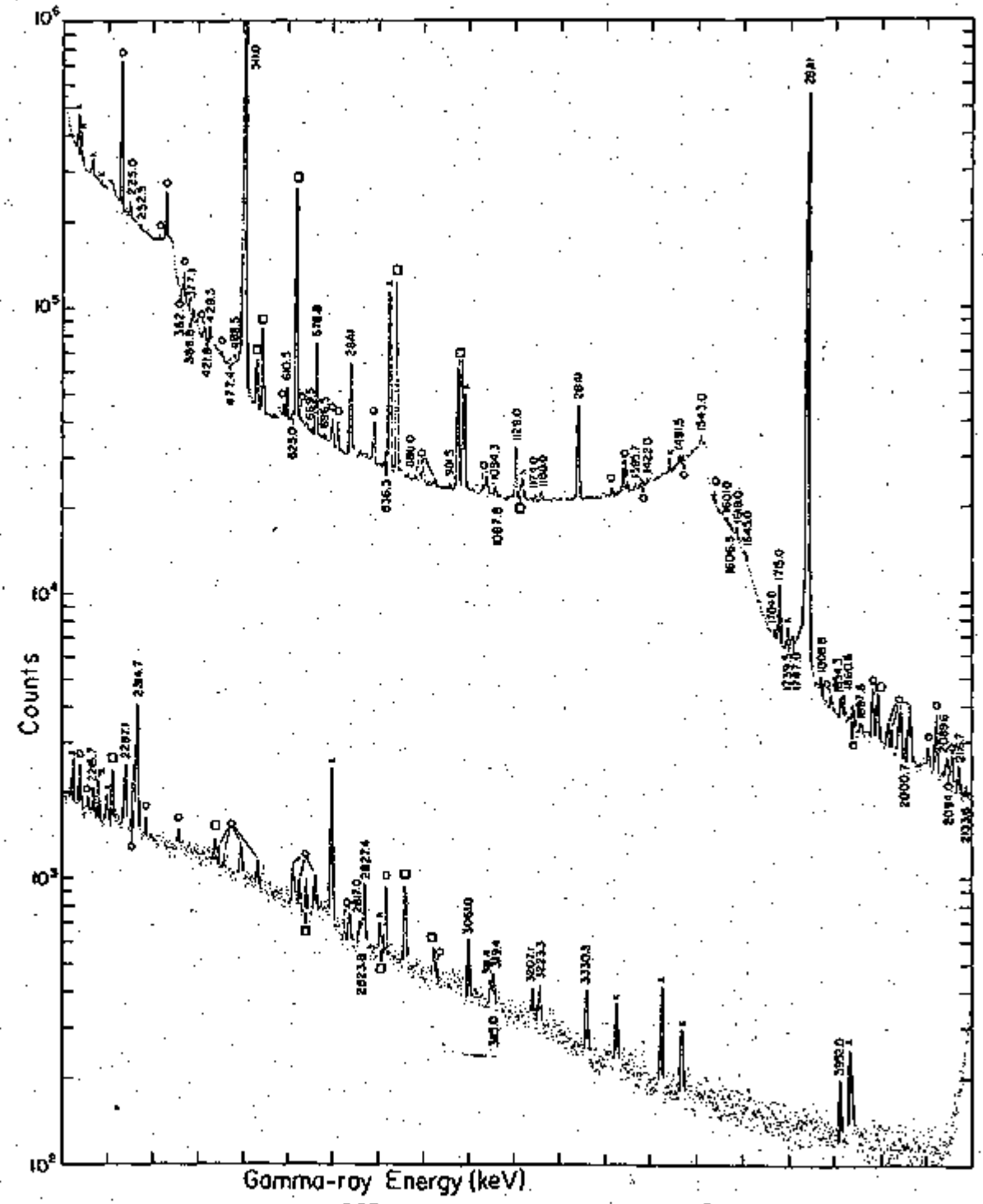

Figure 1. Gamma-ray spectrum of ^{107}Sn produced in a 34-MeV ^{3}He ion bombardment of ^{106}Cd. The peaks attributed to ^{107}Sn decay are labeled with the gamma-ray energy. Peaks labeled with the symbols ○, □, and X belong to ^{107}In, ^{106}In and any unidentified species, respectively.

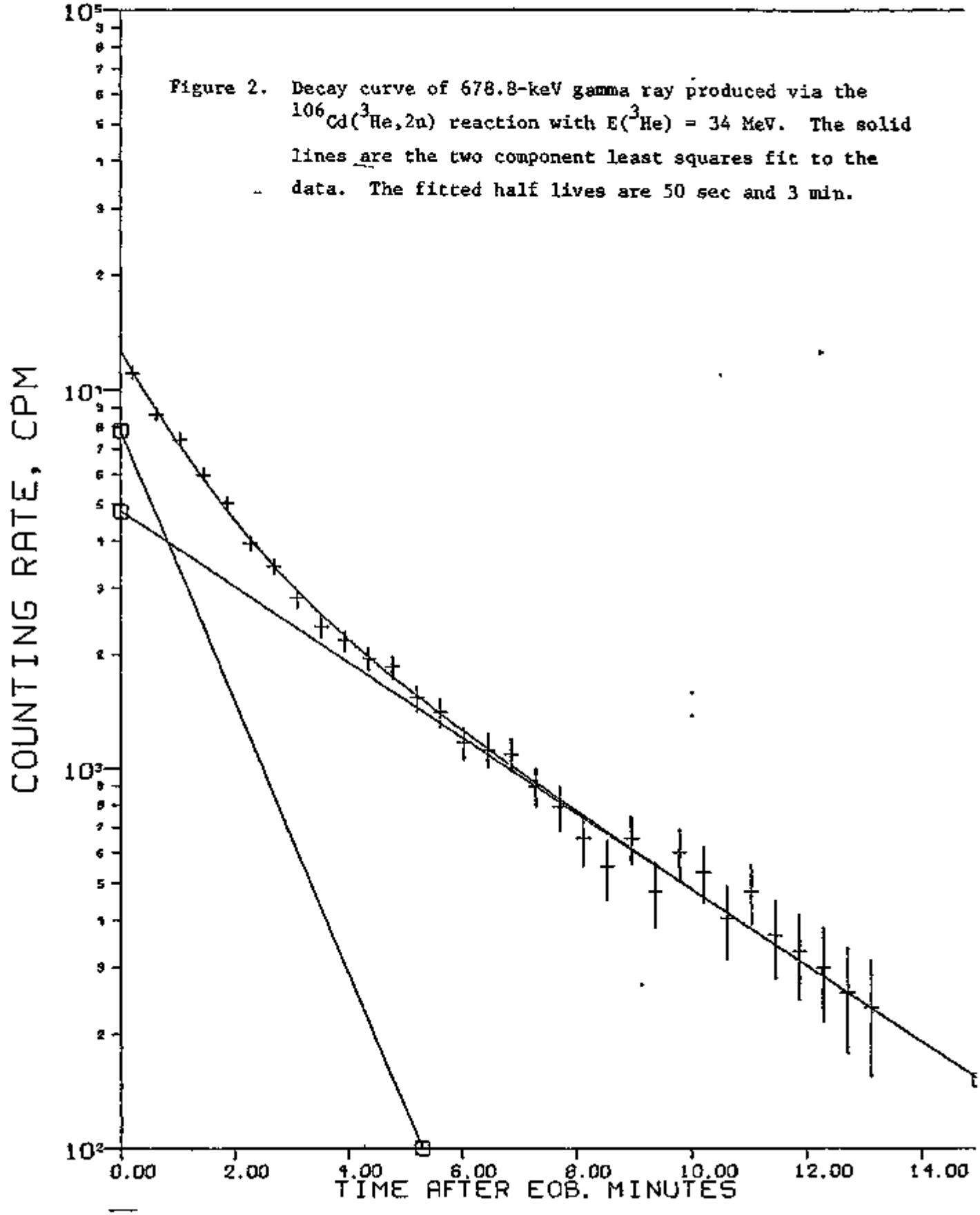

Figure 2. Decay curve of 678.8-keV gamma ray produced via the $^{106}Cd(^{3}He,2n)$ reaction with $E(^{3}He)$ = 34 MeV. The solid lines are the two component least squares fit to the data. The fitted half lives are 50 sec and 3 min.

Table I

Energies and Intensties of γ rays Assigned to the Decay of ^{107}Sn Decay

E_γ [a]	I_γ [b]	E_γ [a]	I_γ [b]
225.0	37.2	1645.0	2.4
252.5	5.4	1704.0	3.6
362.0	16.4	1715.5	10.5
377.1	7.3	1739.5	5.9
386.8	9.1	1747.0	6.7
421.8	5.3	1808.8	9.0
428.5	28.5	1854.3	5.7
477.4	8.1	1860.6	2.9
488.5	13.3	1897.8	6.8
610.5	22.3	2000.7	12.4
625.0	12.7	2088.9	7.0
669.5	6.1	2094.0	6.9
678.8		2116.7	12.0
696.5	1.75	2133.6	2.9
836.0	26.2	2215.7	5.0
888.0	6.6	2287.1	7.8
981.5	5.4	2314.7	69.6
1084.3	9.0	2817.0	1.6
1087.8	4.8	2823.8	2.8
1129.0	100	2827.4	9.7
1174.0	10.7	3061.0	6.4
1188.0	25.0	3111.4	1.4
1395.7	14.5	3115.0	1.2
1422.0	4.5	3119.4	1.8
1491.5	16.9	3207.1	1.1
1543.0	16.6	3223.3	1.5
1601.0	10.8	3330.3	5.9
1606.5	3.5	3952.0	2.2
1618.0	11.2		

[a] Uncertainty in E_γ is ±0.5 keV for E_γ < 1 MeV, and ±1.0 keV for E_γ > 1 MeV.

[b] Uncertainty in intensity is ±5% for I_γ > 15, ±10% for 0.5 < I_γ <15, and ±20% for I_γ < 0.5.

of 3-min and 50-sec as determined by the least squares code CLSQ.[4]

In order to determine if the 678.8-keV γ ray is the ^{107m}In isomeric transition, ^{107}In was produced via the ^{107}Ag(^{3}He,3n) reaction by bombarding natural silver with 30-MeV ^{3}He particles. Note that in this reaction no tin isotopes can be produced. The decay of 678.8-keV γ ray was observed in this experiment and had a single 50-sec component as shown in Fig. 3. This evidence suggests the existence of a 678.8-keV isomeric state in ^{107}In with $t_{1/2}$ = 50 sec and that the half life of the ^{107}Sn ground state is 3 min.

Gamma-gamma coincidence spectra of ^{107}Sn γ rays were obtained using 5-1/2% and 7% Ge(Li) detectors. The data from this experiment is summarized in Table II. A decay scheme shown in Fig. 4 was constructed incorporating 39 of the 57 γ-ray transitions with half lives near 3 min seen in the singles measurements and using the γ-γ coincidence relationships.

B. Decay of ^{106}Sn

The half life of ^{106}Sn was predicted to be ≥1 min.[1] The decay of ^{106}Sn produced via the ^{106}Cd(^{3}He,3n) reaction (Q = -19.3 MeV) with ^{3}He ion bombarding energies of 30 and 34 MeV has been studied using γ-ray spectroscopy. Reaction products were transported from the cyclotron irradiation chamber to a remote low-background area in less than 1 sec using the helium jet recoil transport system. Sources were collected on magnetic tape and moved in front of 6.7% Ge(Li)/with 1.7-keV resolution at 1332 keV using the crystal

4. J.B. Cumming, U.S. Atomic Energy Commission Report No. NAS-NS-3107, p. 25 (1963). Modification E written at Washington University (St. Louis) by A.E. Norris, B.E. Erdal, M.M. Fowler, R.G. Strickert and A.C. Wahl (1974).

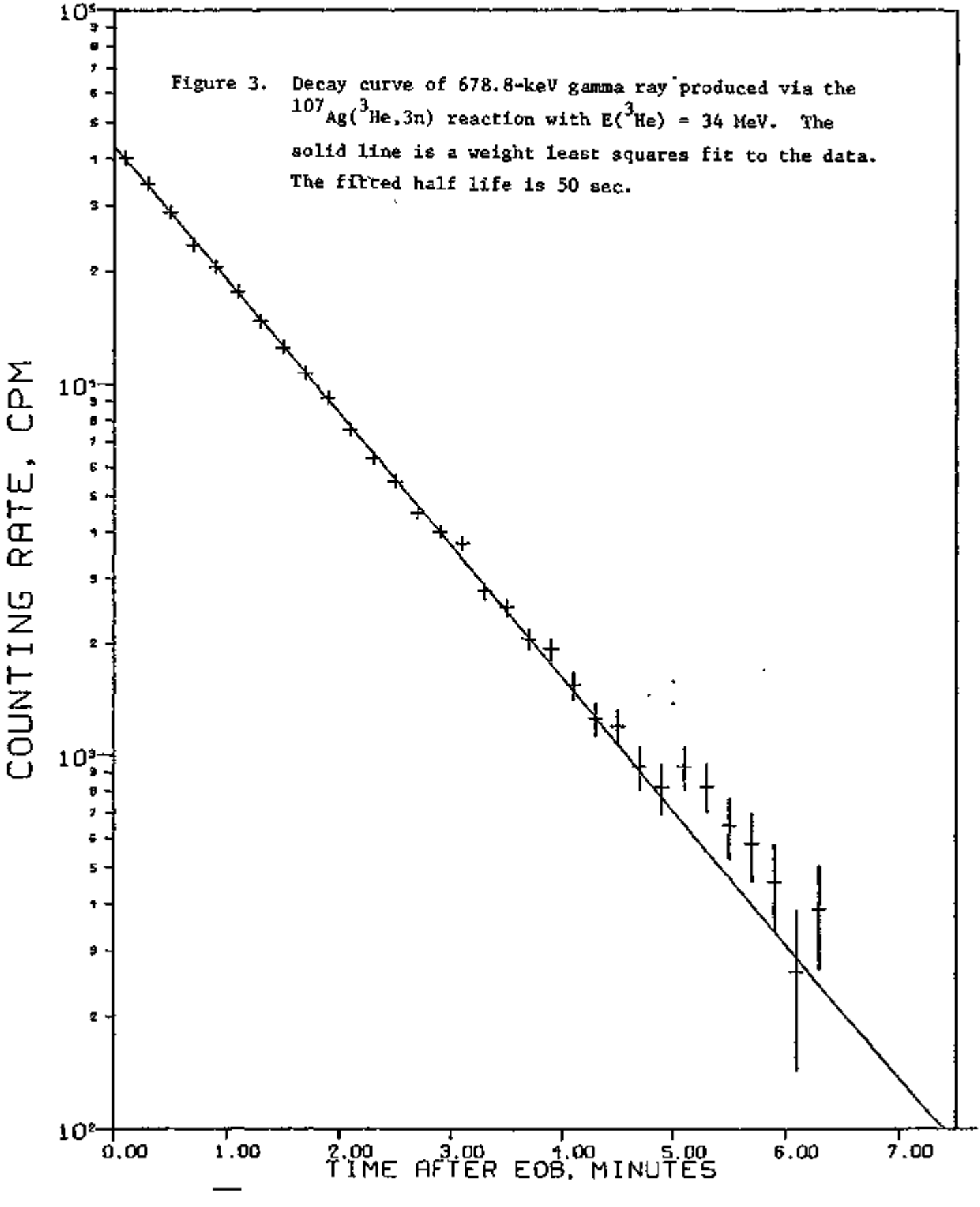

Figure 3. Decay curve of 678.8-keV gamma ray produced via the $^{107}Ag(^{3}He,3n)$ reaction with $E(^{3}He)$ = 34 MeV. The solid line is a weight least squares fit to the data. The fitted half life is 50 sec.

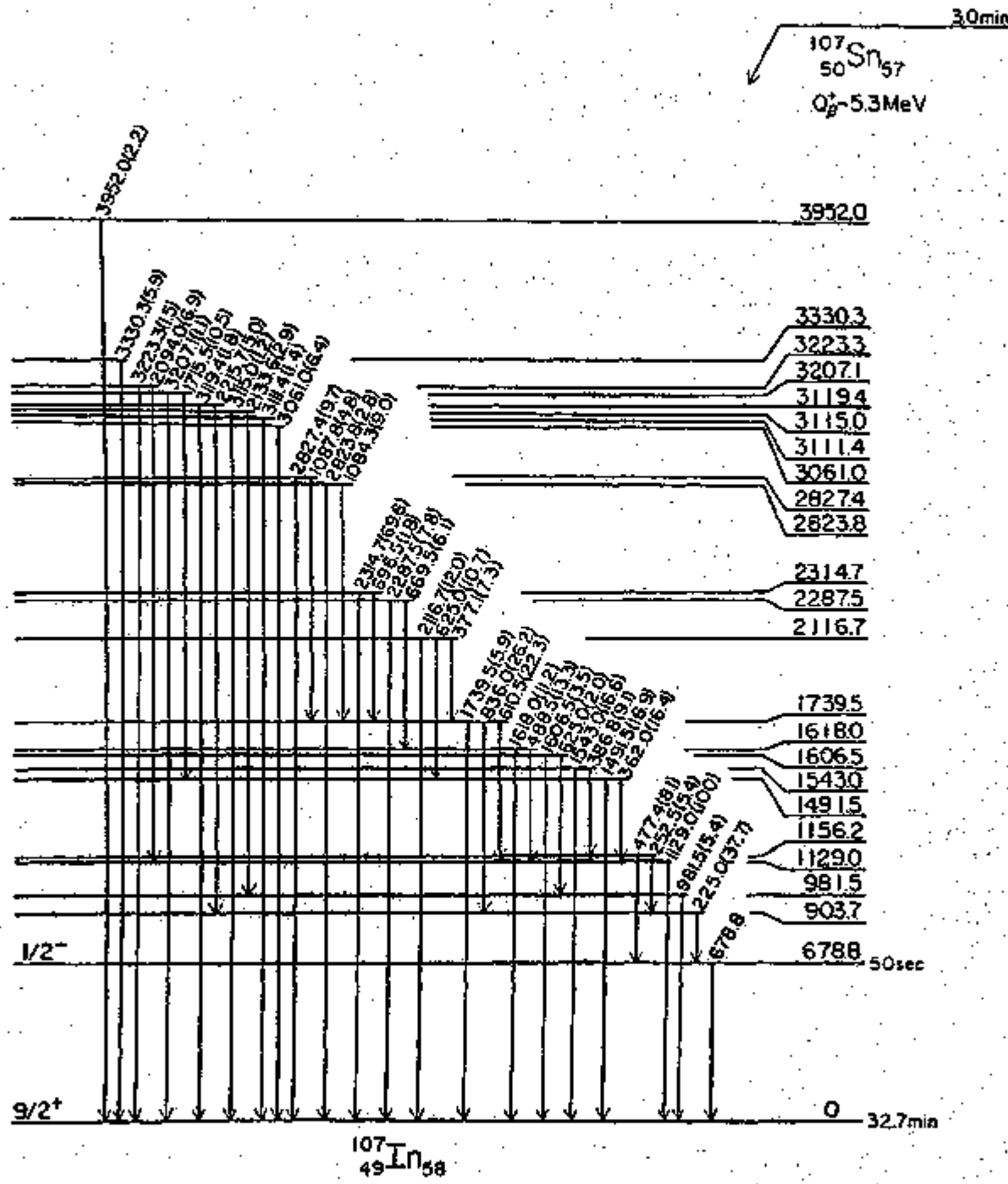

Figure 4. Decay scheme of ^{107}Sn.

Table II

Results of ^{107}Sn γ-γ Coincidence Measurements

γ-ray Gate (keV)	Coincident γ rays (keV)
225.0	252.5,836.0,386.8
252.5	225.0,386.8
362.0	1129.0
386.8	225.0,252.5,477.4
477.4	386.8
488.5	1129.0
610.5	1129.0
625.0	981.5
836.0	225.0
981.5	625.0
1129.0	362.0,488.5,610.5

tape transport system. A strong transition at 133.5 keV with 10 ± 2-sec half life was seen only in 34-MeV ^{3}He ion bombardments which may belong to ^{106}Sn decay. Three additional transitions with 30 ± 5-sec half-lives were also seen in these bombardments.

(H.-C. Hseuh and E. S. Macias)

C. Decay of 10.8-Min ^{108}Sn

Although the half-life of ^{108}Sn has been known for some time,[5,6] no high resolution γ-ray spectrum or detailed decay scheme incorporating γ-γ coincidence information has been reported for the decay of ^{108}Sn.[7] We are studying ^{108}Sn as part of our study of nuclides near closed shells. The ^{108}Sn sources were produced via the ^{106}Cd(^{4}He,2n) reaction by bombarding a 95.5% enriched ^{106}CdO target with E_{α} = 30 MeV. The activity was transported to a low background area with the Washington University helium jet recoil transport system. Anti-Compton and direct γ-ray spectra and γ-γ coincidence spectra have been studied using 5, 7 and 12% Ge(Li) detectors. A total of 22 γ rays listed in Table III have been assigned to the decay of 10.8 ± 0.3-min ^{108}Sn on the basis of their half lives.

Results of the γ-γ coincidence experiment are now being analysed in order to construct a comprehensive decay scheme of ^{108}Sn.

(H.-C. Hseuh and E. S. Macias)

D. Decay of Short-Lived Palladium Isotopes: ^{97}Pd and ^{96}Pd

The study of the level structure of $^{97}_{45}Rh_{51}$ and $^{96}_{45}Rh_{52}$ populated via the decay of short-lived palladium isotopes was begun during the past year as

---

5. W. Mead, Ph.D. Thesis, University of California (1956): UCRL-3488 (1956).
6. B.G. Kiselev, V.R. Burmistrov, Sov. J. Nucl. Phys. 11, 137 (1970).
7. F.E. Bertrand, Nucl. Data Sheets B7, 33 (1972).

Table III

Energies and Intensities of 10.8-min ^{108}Sn γ rays

E_γ(keV)	I_γ
105.0 ± 0.5	26.5 ± 0.3
169.4 ± 0.1	32.3 ± 0.3
237.1 ± 0.1	9.6 ± 0.3
273.6 ± 0.3	65.9 ± 0.4
363.5 ± 0.5	1.2 ± 0.2
397.4 ± 0.4	100
423.1 ± 0.1	3.3 ± 0.3
669.9 ± 0.3	23.3 ± 0.5
829.3 ± 0.2	4.2 ± 0.7
847.5 ± 0.6	3.3 ± 0.6
858.3 ± 0.3	3.5 ± 0.7
889.4 ± 0.6	5.7 ± 0.4
950.3 ± 0.3	2.9 ± 0.4
976.9 ± 0.2	4.7 ± 0.4
1129.0 ± 0.3	7.2 ± 0.5
1375.1 ± 0.3	1.8 ± 0.4
1430.7 ± 0.7	2.6 ± 0.5
1714.4 ± 0.3	3.7 ± 0.6
1825.4 ± 0.3	3.2 ± 0.6
1890.6 ± 0.3	5.2 ± 0.4
1943.9 ± 0.8	4.1 ± 0.4
2028.6 ± 0.4	4.0 ± 0.4

part of our study of nuclei near closed shells. The identification of 3.3 ± 0.3-min ^{97}Pd was first reported by Aten and Kapteyn[8] in 1969. That is the only investigation of ^{97}Pd decay which has been reported;[9] no information about the identifcation of ^{96}Pd has been reported.[10]

We have produced ^{97}Pd via the ^{96}Ru(^{3}He,2n) reaction by bombarding 95% enriched ^{96}Ru with 30-MeV ^{3}He ions. The Washington University helium jet system was used for transporting the activity to a 12% Ge(Li) detector. We have identified several γ rays which we attribute to the decay of 3.3-min ^{97}Pd. Experiments are in progress to determine low intensity transitions following the decay of ^{97}Pd and to identify ^{96}Pd.

(E. Jensen, L. Zapata, and E. S. Macias)

E. Decay of 5.8-Min ^{140m}Pm and 10-Sec ^{140g}Pm to Levels of ^{140}Nd

During the past year this investigation has been completed and the results are presented in the accompanying preprint which has been submitted to The Physical Review. The abstract from that paper is given below:

> The nuclear level structure of ^{140}Nd has been investigated by studying the decay of 5.8-min ^{140m}Pm and 10-sec ^{140g}Pm with Ge(Li) γ-ray detectors. Sources were produced via the ^{141}Pr(^{3}He,4n) reaction. The study of ^{140g}Pm decay utilized a helium-jet recoil transport system. Fourteen γ rays were assigned ^{140}Pm decay and nine were attributed to ^{140g}Pm decay (see Tables IV and V). Decay schemes of ^{140m}Pm and ^{140g}Pm were constructed (Fig. 5). Evidence for the low-spin members of the two-phonon triplet in ^{140}Nd is also presented.

(M. R. Zalutsky and E. S. Macias)

---

8. A.H.W. Aten, Jr. and J.C. Kapteyn, Radiochim. Acta 12, 218 (1969).
9. L.R. Medsker, Nucl. Data Sheets 10, 1 (1973).
10. L.R. Medsker, Nucl. Data Sheets 8, 599 (1972).

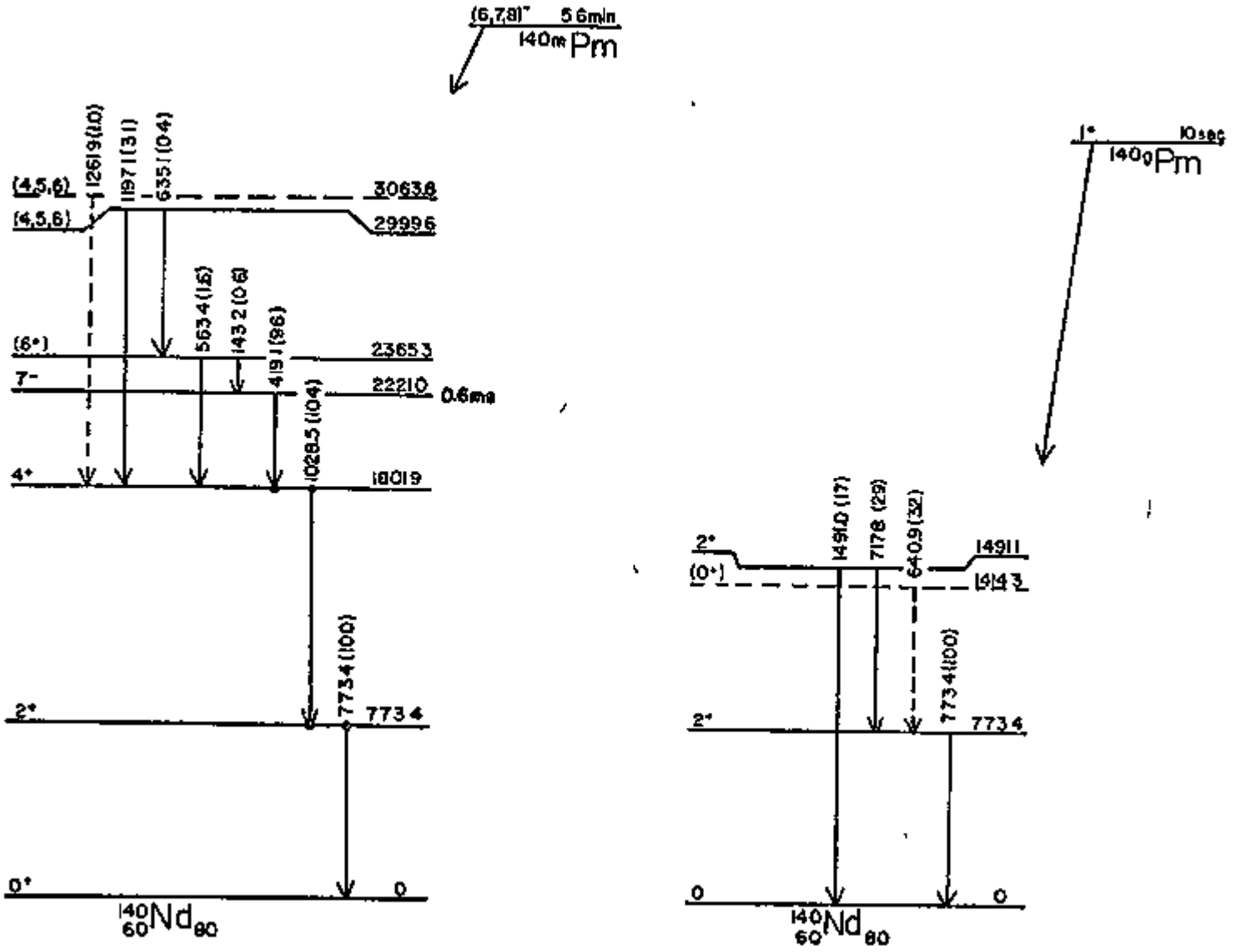

Figure 5. Levels of ^{140}Nd populated in the β decay of ^{140m}Pm and ^{140g}Pm.

Table IV. Energies and relative intensities of γ rays observed in ^{140m}Pa decay

Energy (keV)[a]	Relative intensity
143.2	0.6 ± 0.2
257.9	1.4 ± 0.8
419.1	96 ± 4[b]
563.4	1.6 ± 0.4
635.1	0.4 ± 0.2
651.8	0.5 ± 0.3
773.4	100
880.4	0.5 ± 0.4
1028.5	104 ± 6
1110.9	0.3 ± 0.2
1197.7	3.1 ± 0.7
1261.9	1.0 ± 0.3
1733.8	0.3 ± 0.1
1837.8	0.2 ± 0.1

[a]The uncertainties in energy are ±0.2 keV for $I_\gamma > 90$ and ±0.4 keV for $I_\gamma < 90$.

[b]Corrected for internal conversion using α_T = 0.057 as calculated from R. S. Hager and E. C. Seltzer, Nucl. Data Tables, A4, 1 (1968).

Table V. Energies and relative intensities of γ rays observed in ^{140g}Pa decay

Energy (keV)[a]	Relative intensity
159.8	19 ± 5
477.1	51 ± 10
640.9	32 ± 6
717.8	29 ± 9
773.4	100 ± 20
1013.8	14 ± 4
1138.7	30 ± 11
1204.8	37 ± 8
1491.0	17 ± 3

[a]The uncertainties in energy are ±0.3 keV.

F. Structure of N = 81 Nuclei: Levels of ^{141}Nd and ^{139}Ce Populated in Beta Decay

The levels of $^{141}_{60}Nd_{81}$ and $^{139}_{58}Ce_{81}$, nuclei with a single hole in the N = 82 neutron shell, are of particular interest because they are expected to be well characterized by the particle-core coupling model. Calculations using this model have been performed for N = 81 nuclei[11] however these calculations can not account for the large number of levels below 2 MeV seen in $^{135}_{54}Xe_{81}$.[12] The study of N = 81 isotones has been extended to ^{141}Nd and ^{139}Ce to study these levels in higher Z nuclides to see if the discrepancy with theory exists as the proton orbitals become fuller.

This work has been completed and will be submitted for publication shortly. An abstract of the work is given below.

> The nuclear level structure of ^{141}Nd and ^{139}Ce has been investigated by studying the decay of 20.9-min ^{141}Pm produced via the ^{141}Pr(^{3}He,3n) reaction and the decay of 4.5-hour ^{139}Pr produced by the ^{140}Pr(γ, n) reaction. Anti-Compton gamma-ray spectra were taken as a function of time in order to confirm assignment of the ^{141}Nd and ^{139}Ce gamma rays (see Fig. 6). For the ^{141}Pm decay, anti-Compton and gamma-gamma coincidence measurements were used to deduce a decay scheme that includes nine previously unreported levels in ^{141}Nd and incorporates 67 of the 70 gamma rays attributed to the decay of ^{141}Pm (see Figs. 7 and 8). The results of this work are compared to recent measurement in the N = 81 isotones.

The study of ^{139}Pr decay was performed in collaboration with R. A. Meyer of Lawrence Livermore Laboratory.

(M. R. Zalutsky, E. S. Macias, R. A. Meyer)

---

11. Heyde and Brussard, Z. Phys. 259, 15 (1973).

12. E.S. Macias and W.B. Walters, Nucl. Phys. A169, 305 (1971).

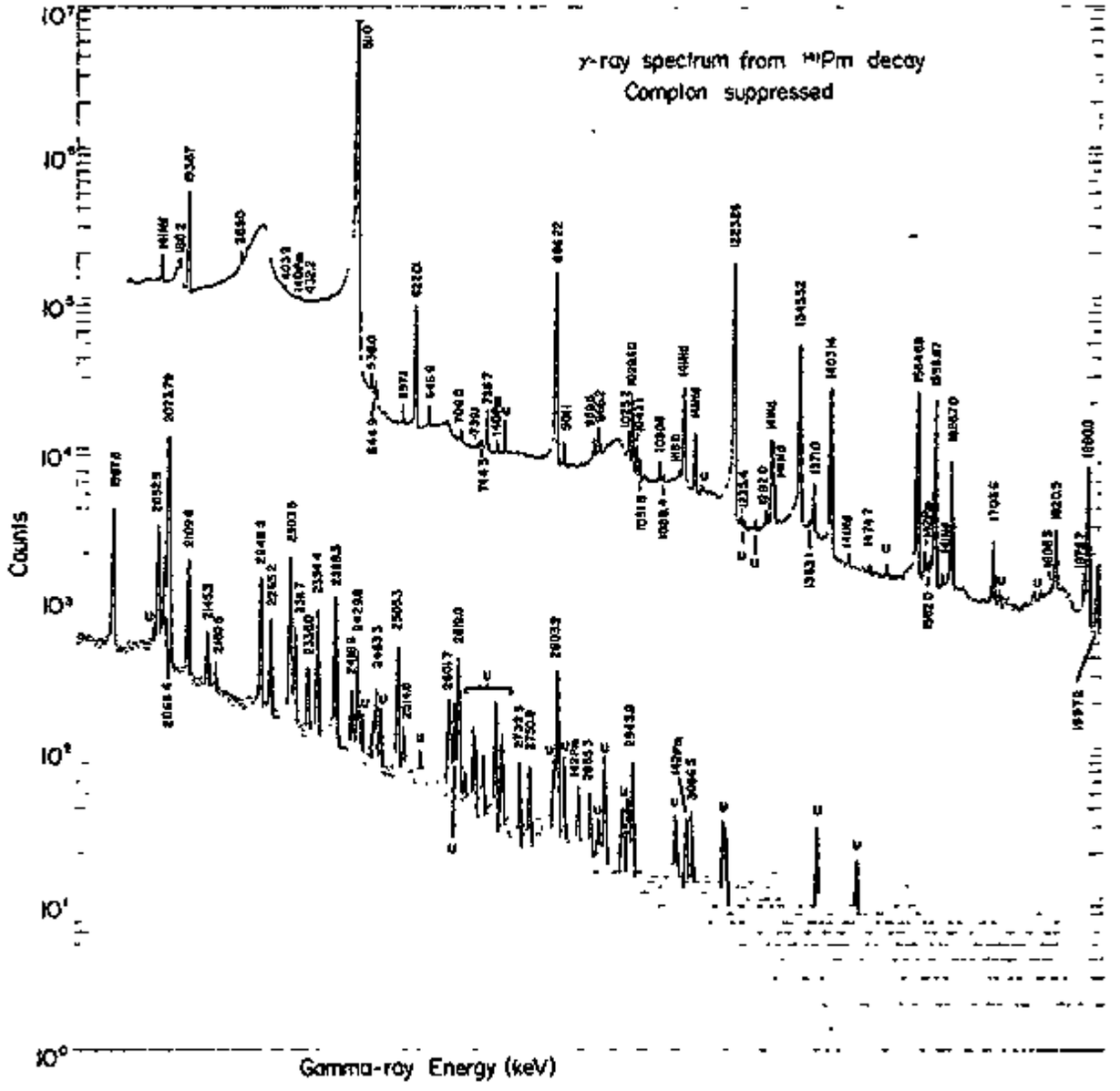

Figure 6. Spectrum of ^{141}Pm γ-rays taken with the anti-Compton spectrometer.

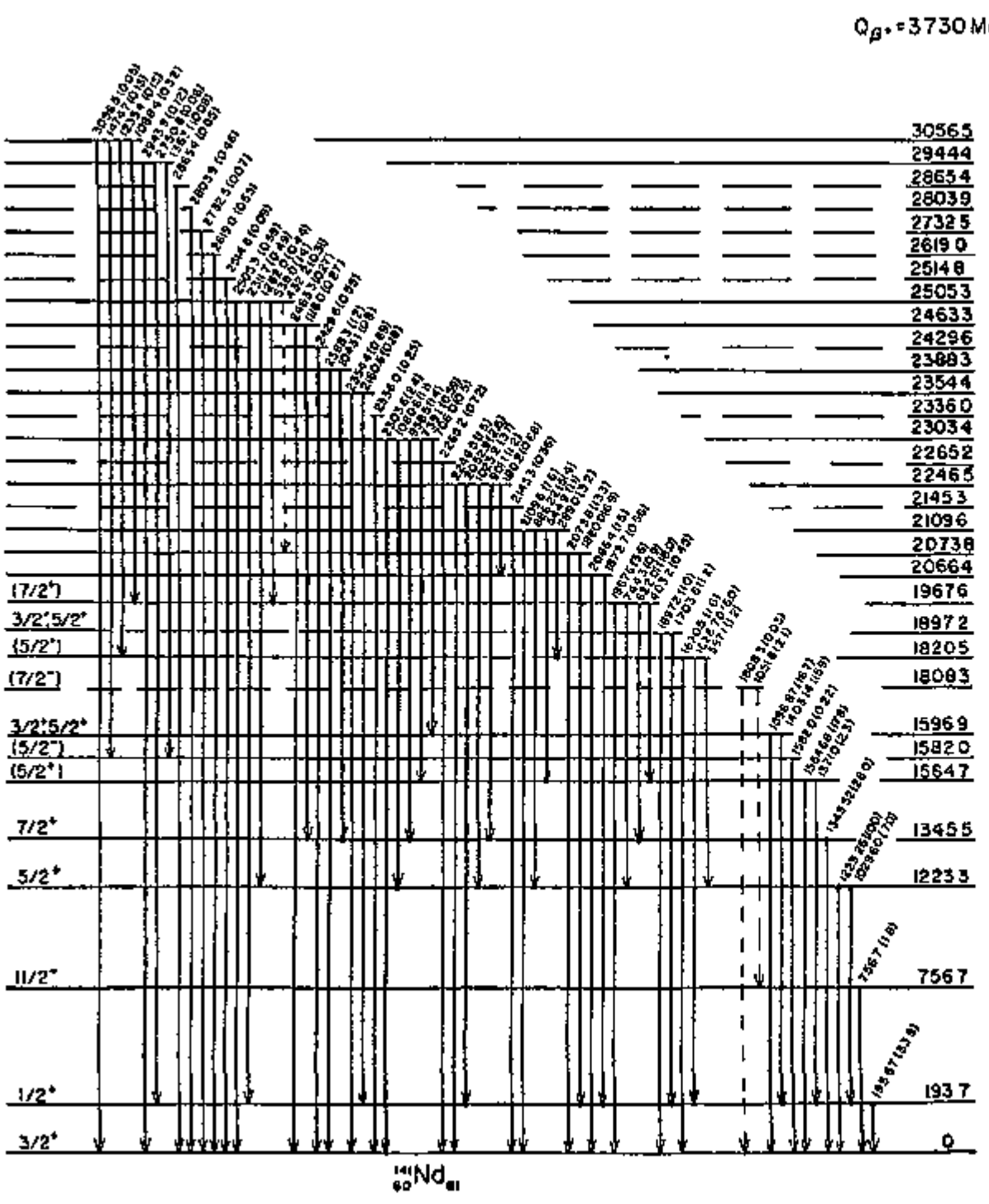

Figure 7. Decay scheme of $^{141}_{61}Pm$. The energy scale is not linear.

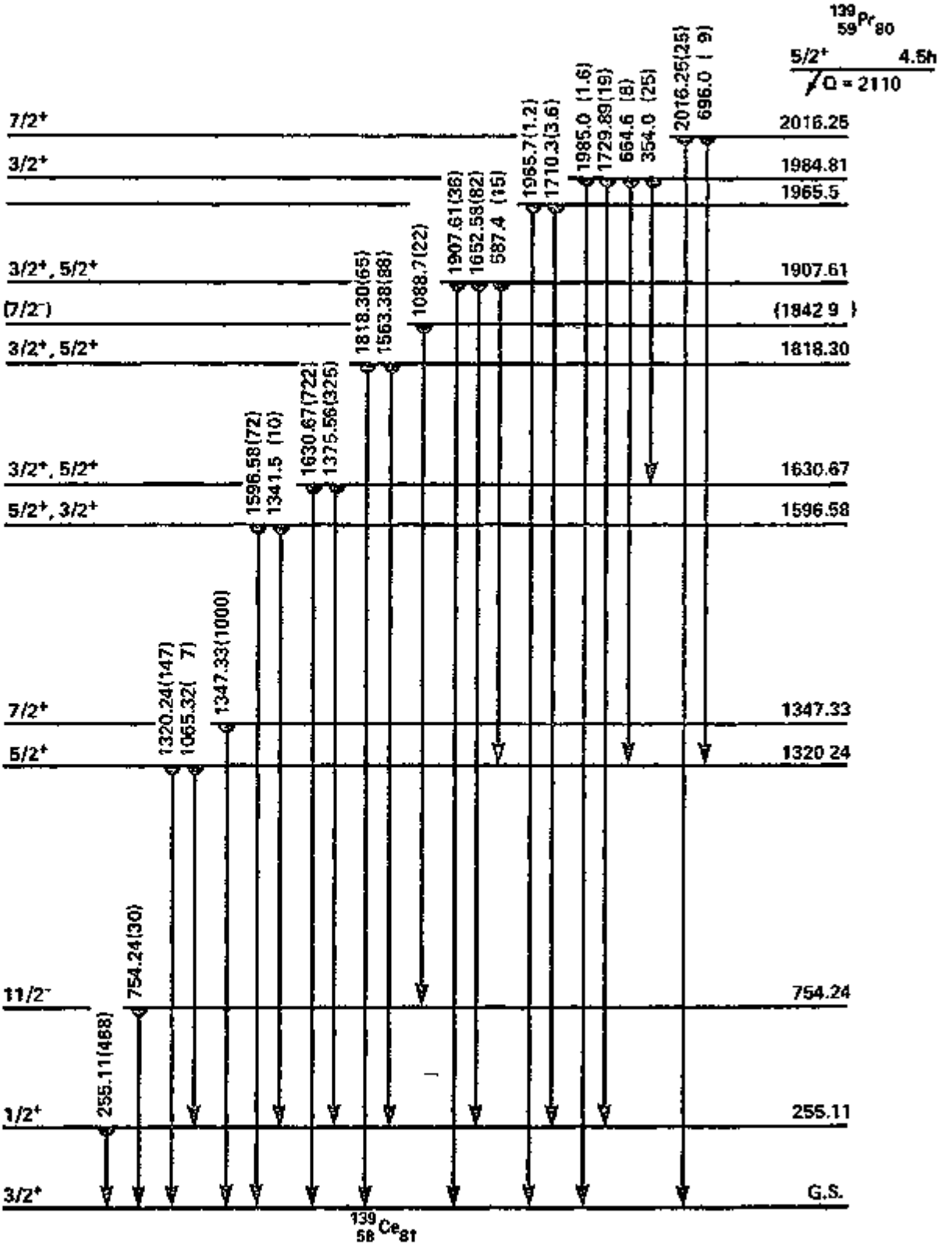

Figure 8. Decay scheme of ^{139}Pr.

G. Decay of $^{89m+g}Nb$

As part of our investigation of nuclei near closed shells we are continuing our study of the levels of $^{89}_{49}Zr_{40}$ populated in the decay of 66-min ^{89m}Nb and 122-min ^{89g}Nb. Analysis of the anti-Compton γ-ray spectrum indicates many previously unreported γ rays. The results of a γ-γ coincidence experiment are presently being analysed in order to construct a coherent level scheme for ^{89}Zr.

(D. A. Simon and E. S. Macias)

H. Decay of ^{149}Pm and ^{149}Eu to Levels of ^{149}Sm

This work has been completed and is being prepared for publication. This work was performed in collaboration with R. A. Meyer of Lawrence Livermore Laboratory.

(E. S. Macias and R. A. Meyer)

I. Search for an Anisotropy between Lℓ X Rays and γ Rays Emitted following the Decay of ^{243}Cm

This work has been completed and the results are presented in the accompanying preprint which has been submitted for publication in The Physical Review. The abstract of that paper is given below:

> The anistropy of Lℓ x rays and γ rays of ^{239}Pu following the decay of ^{243}Cm has been investigated. A Ge(Li) crystal with 250-eV resolution at 5.9 keV was used to detect Lℓ x rays. A NaI(Tl) crystal was used to detect six γ rays between 210 and 285 keV. The measured anisotropy is $A = (3 \pm 6) \times 10^{-3}$. This is less than 2% of the maximum predicted anisotropy assuming that the magnetic substate alignment has been completed retained in the coupling of cascade γ rays and x rays.

(M. R. Zalutsky and E. S. Macias)

II. In-Beam γ-Ray Spectroscopy

A. Lifetime Measurements of Low-Lying Levels in ^{93}Mo Populated via the ^{93}Nb(p,nγ) Reaction using the Doppler Shift Attenuation Method

The nucleus ^{93}Mo, is a relatively simple "shell model" nucleus. With only one neutron outside the major shell closure at N = 50. Auerbach and Talmi[13] have argued quite convincingly that the important proton configurations of the low-lying states are $p_{1/2}^2\ g_{9/2}^2$ and $g_{9/2}^4$, and that seniority is conserved to a good approximation. They have computed the spectrum of ^{93}Mo using only the $p_{1/2}^2\ g_{9/2}^2\ d_{5/2}$ and $g_{9/2}^4\ d_{5/2}$ configurations, and are able to explain the "spin gap" which results in the 6.9 hr. $21/2^+$ isomer at 2425 keV in ^{93}Mo. The energies of the $13/2^+$ and $9/2^+$ levels which participate in the γ-ray cascade deexciting the 6.9 hr. isomer are also well described by their model. However, many levels are not accounted for in these calculations. A more complete description of this nucleus requires the inclusion of more neutron orbitals in the model space. The importance of higher neutron orbitals can be estimated by examining the work of Hughes[14] in which he calculates the spectrum of ^{89}Sr taking into account the $2d_{5/2}$, $3s_{1/2}$, $2d_{3/2}$, and $1g_{7/2}$ neutron orbitals. His results indicate that all of these orbitals are important in describing states below 3 MeV of excitation. Although there exist codes that could handle the resulting large basis set, there are apparently technical difficulties in handling the $g_{9/2}$ orbital.

Choudhury and Clemens[15] have employed an intermediate coupling model to compute the spectrum of the low-lying even parity levels in ^{93}Mo. The

---

13. N. Auerbach and I. Talmi, Nucl. Phys. 64, 458 (1965).

14. T.A. Hughes, Phys. Rev. 181, 1586 (1969).

15. D.C. Choudhury and J.T. Clemens, Nucl. Phys. A125, 140 (1969).

extra core neutron is assumed to occupy the $2d_{5/2}$, $1g_{7/2}$, and $3s_{1/2}$ orbitals, and is coupled to the vibrational states of the ^{92}Mo core. The ^{92}Mo core space is truncated to include up to two-phonon quadrupole excitations. This model gives a good description of the first $1/2^+$, $7/2^+$, $9/2^+$, $3/2^+$ and $5/2^+$ excited states. The $13/2^+$ and $21/2^+$ levels are, however, not predicted.

A further test of the accuracy of the various wave functions would be their ability to predict the transition rates or lifetimes of the nuclear states. Choudhury and Clemens have computed the lifetimes of the first $1/2^+$, $7/2^+$, and $9/2^+$ excited states in ^{93}Mo. However no calculations using a large basic set have been reported for the transition rates of ^{93}Mo.

The fact that the levels in ^{93}Mo can be reached via both the (p,nγ) and (α,2nγ) reactions makes ^{93}Mo an interesting candidate for study. The ^{93}Nb(p,nγ) reaction perferentially populates the lower spin levels in ^{93}Mo, while the ^{91}Zr(α,2nγ) reaction will preferentially populate the higher spin levels. However, the ground state spin of ^{93}Nb is 9/2, while the ground state spin of ^{91}Zr is 5/2. Hence we expect some redundancy of the levels populated in the two reactions. There exist codes[16] with which one may compute the cross sections and alignments for levels populated via the (p,nγ) reaction within the framework of the compound statistical model. For the (α,2nγ) reaction, one usually must resort to more phenomenalogical procedures.[17]. Thus the (p,nγ) reaction provides the preliminary ground work necessary to unambiguously extract information from the more complex (α,2nγ) reaction.

---

16. Eric Sheldon and Richard Michael Strang, Comput. Phys. Commun. 1, 35 (1969).

17. T. Yamazaki, Nucl. Data A3, 1 (1967).

We have measured the lifetimes of many of the low-lying levels in ^{93}Mo populated via the ^{93}Nb(p,nγ) reaction using the Doppler-shift attenuation method. The experiment was performed at proton bombarding energies of 3.7 and 4.4 MeV. Relatively few levels were excited at the lower energy and the results were interpreted in terms of previously observed levels. Many more levels were populated in an experiment carried out at a proton bombarding energy of 4.4 MeV. The anti-Compton γ-ray spectrum for a 4.4 MeV proton bombardment is shown in Figs. 9 and 10. A γ-γ coincidence experiment was performed at 4.4 MeV in order to establish the complete decay scheme of the levels populated which is shown in Fig. 11. We observed 47 levels below 3.07 MeV of excitation, and obtained lifetime information for 40 of these levels listed in Table VI. In Fig. 12, the observed photopeak centroid energy is plotted as a function of the cosine of the angle of emission for the transitions observed in the ^{93}Nb(p,nγ) reaction. The solid line is the least-squares fit to the data. The observed attenuated Doppler-shift, given by the slope of the least-squares fitted line, is indicated in the figure. The results are compared with previous determination where possible. This work has been completed and is being prepared for publication.

(L. L. Rutledge, E. S. Macias and D. G. Sarantites)

B. Lifetime Measurements of Levels in ^{93}Mo via the Recoil Distance Method

As described in the previous section of this report many of the lifetimes of the low lying levels in ^{93}Mo have been determined by the Doppler-shift attenuation method using the ^{93}Nb(p,nγ)^{93}Mo reaction at a proton bombarding energy of 4.4 MeV. However, this technique is not sensitive to lifetimes $\geq$2 psec. We have observed an interesting level at $E^* = 2430$ keV which decays via a 268-keV gamma ray to the $13/2^+$ level at 2162 keV. This

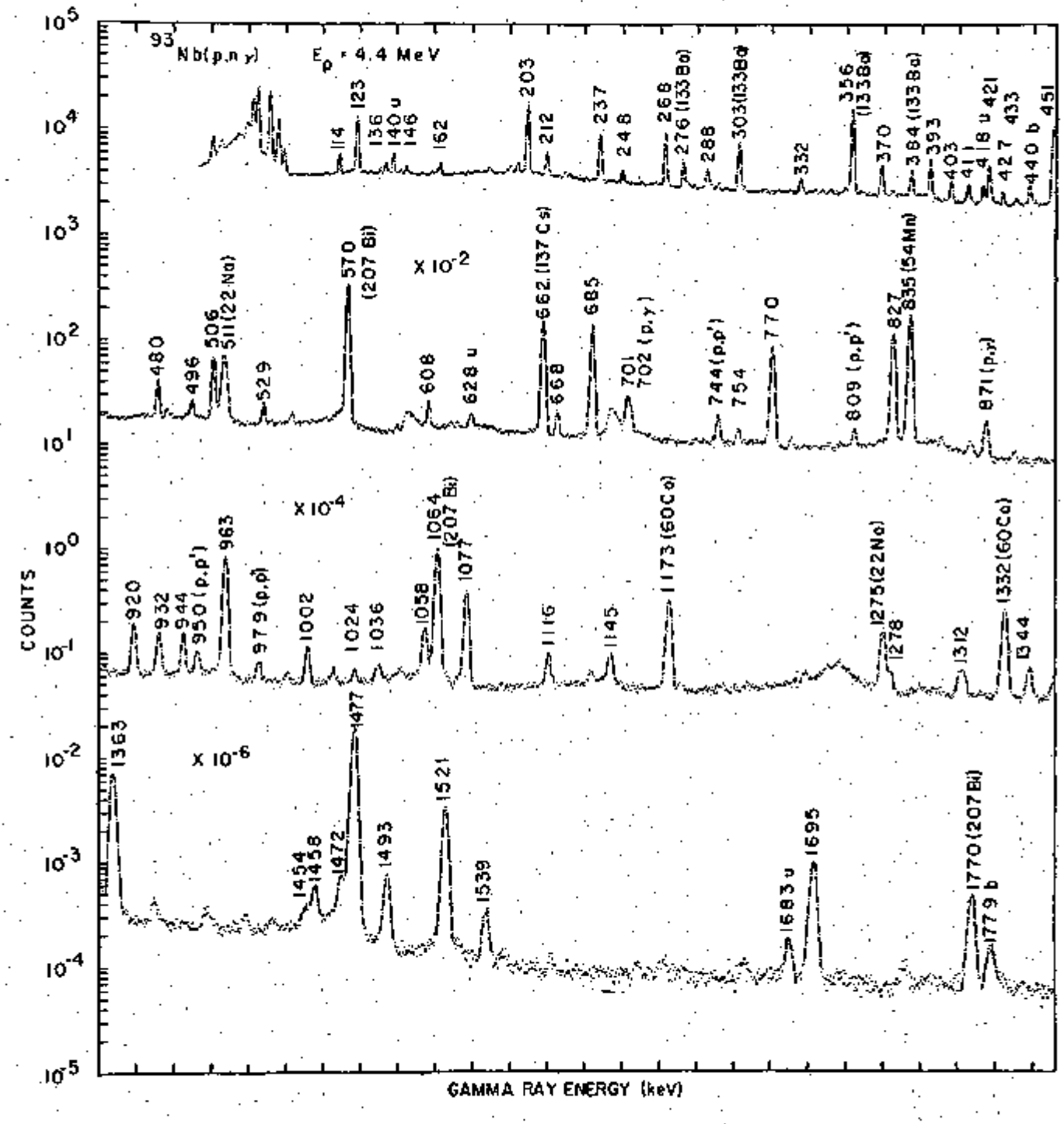

Figure 9. Low-energy anti-Compton γ-ray spectrum from 4.4-MeV proton bombardment of ^{93}Nb.

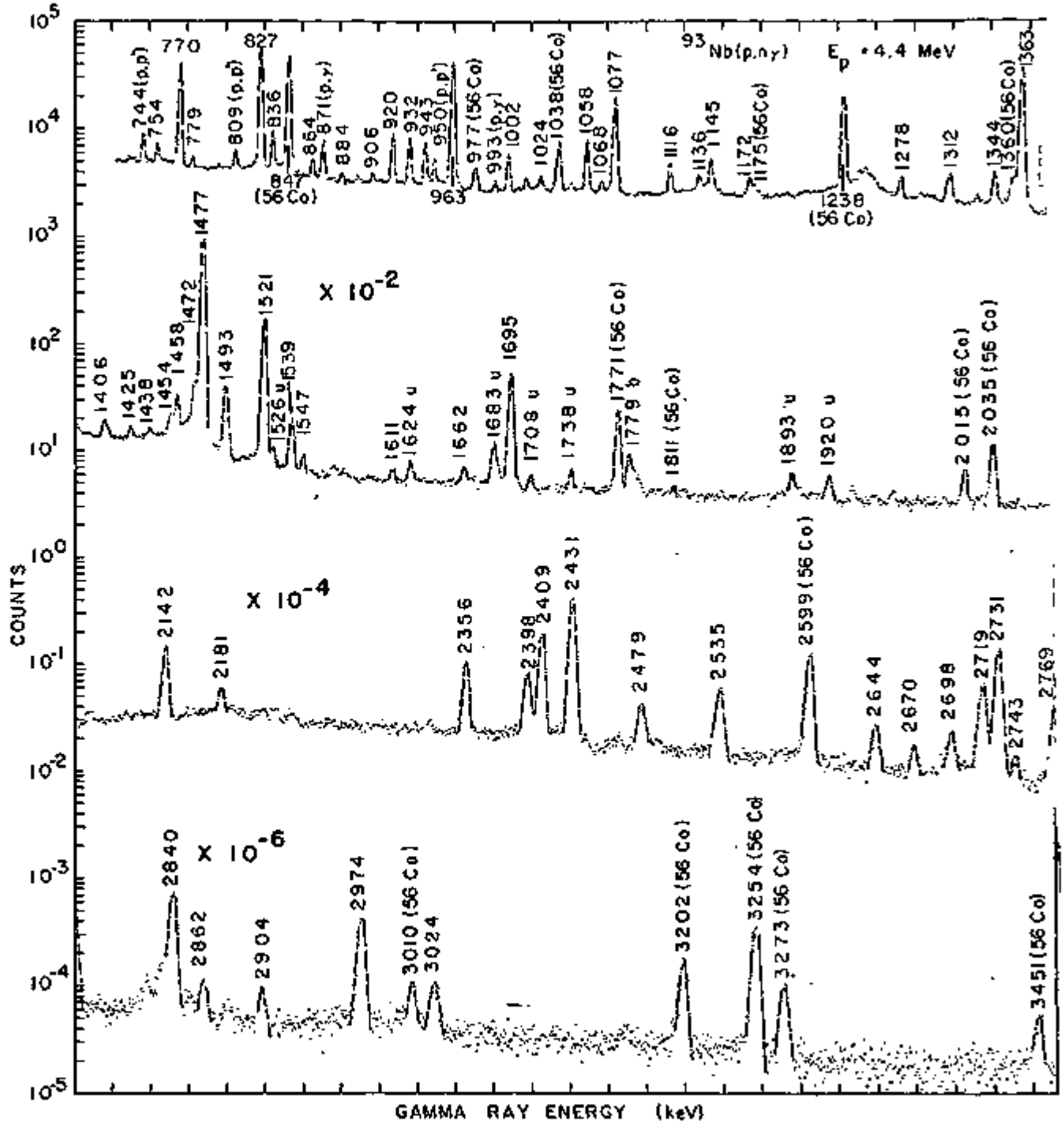

Figure 10. High-energy anti-Compton γ-ray spectrum from 4.4-MeV proton bombardment of ^{93}Nb.

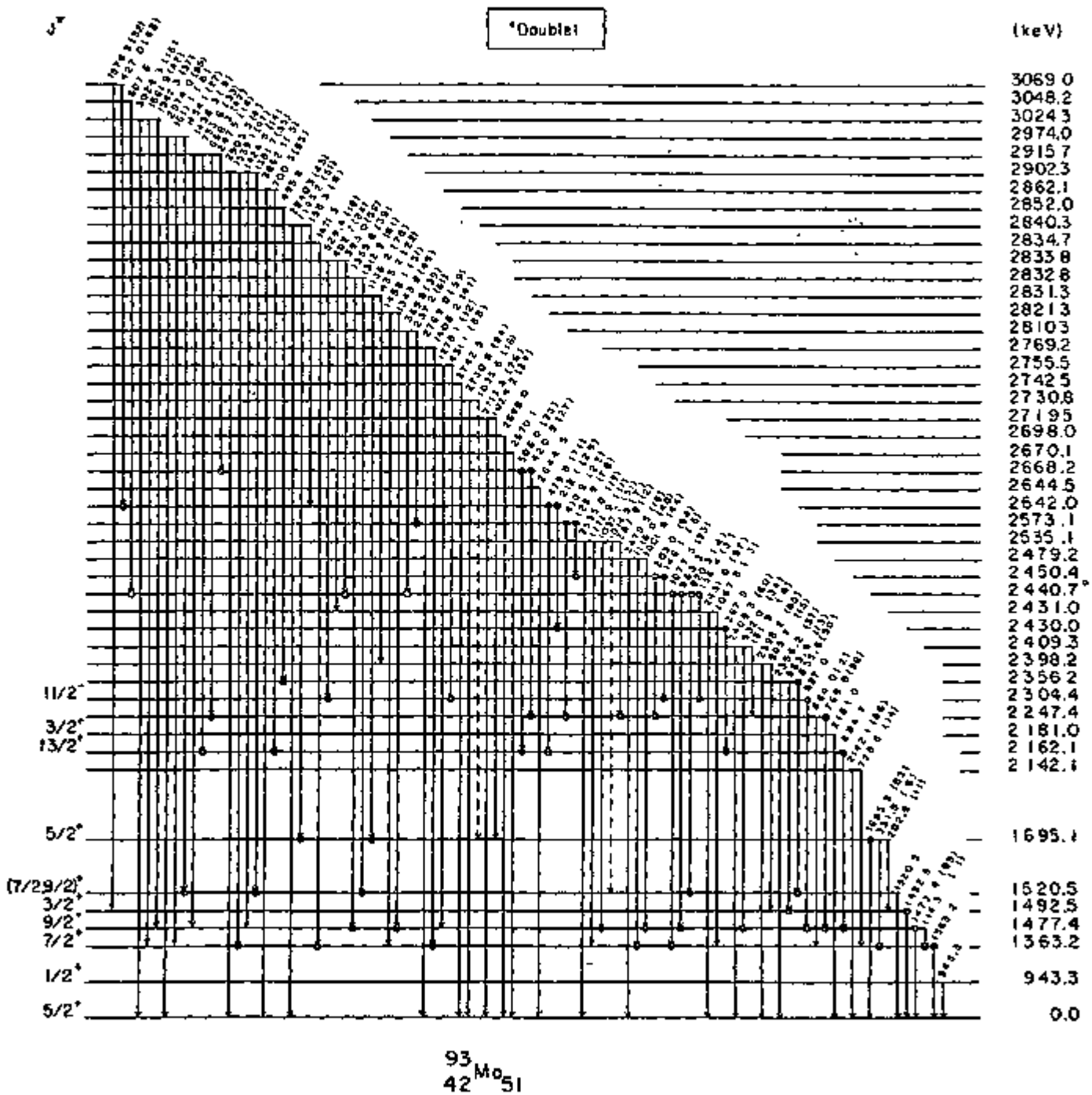

Figure 11. Level scheme of ^{93}Mo.

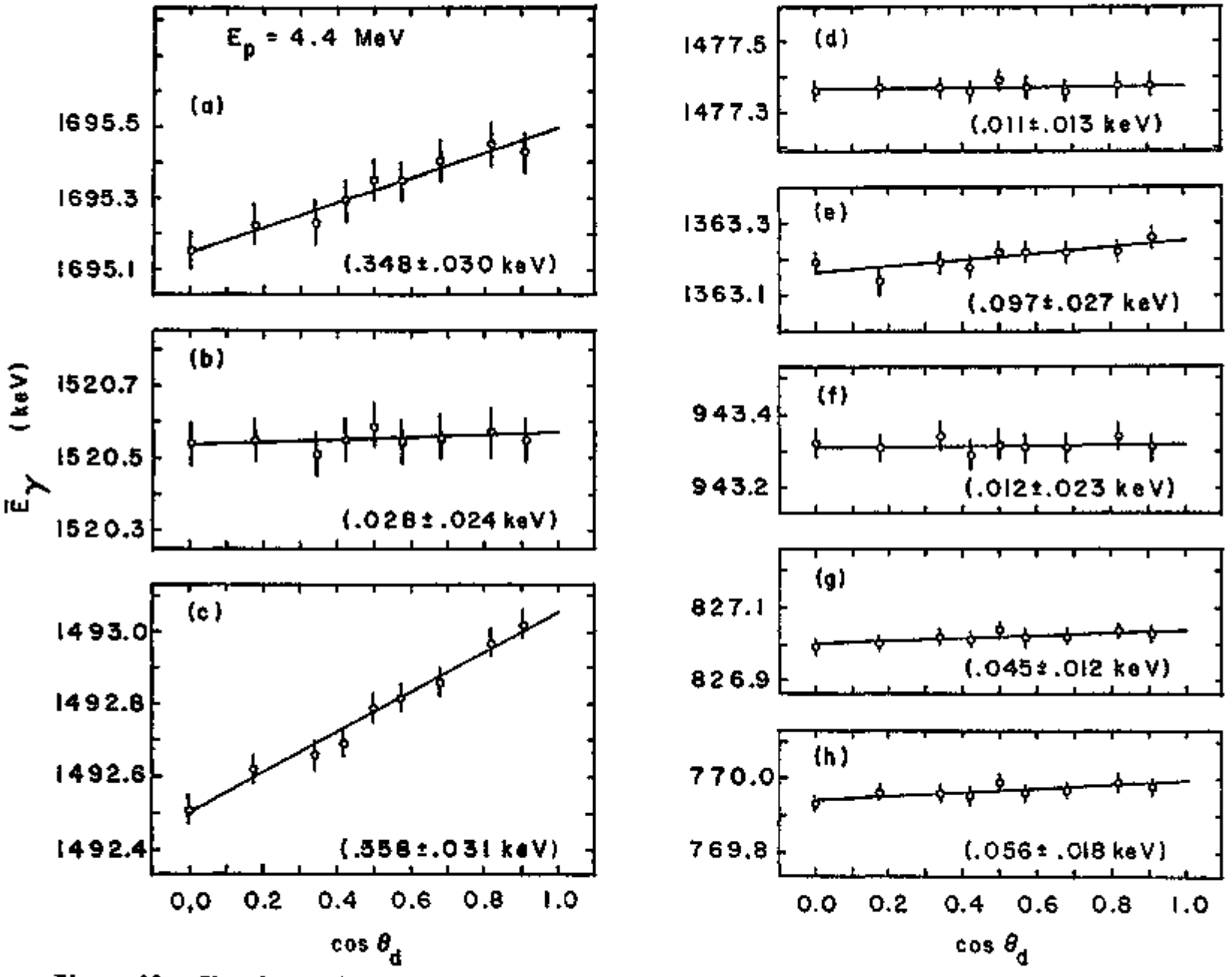

Figure 12. The observed photopeak centroid energy plotted versus the cosine of the angles of emission observed in the ^{93}Nb(p,nγ) reaction. The solid line is the least squares fitted line, th slope of that line is also given.

E_x^* (keV)	E_γ (keV)	Branching Ratio (%)	F(τ)	τ (fs) $(\tau_d = 0)$	$(\tau_d = \infty)$
	2355.2 1	36.9 13	.003 23		
2396.2 1	985.6 3	15.6 33		30 ± 5	
	2398.2 1	84.5 35	.305 48		
2409.3 1	161.9 3	6.1 6		680^{+340}_{-90}	
	932.0 1	34.2 10	.059 20		
	2409.3 2	59.7 29	.855 10		
2430.0 1	267.9 1				
2431.0 2	1087.8 2	7.7 2		175^{+25}_{-20}	
	2431.0 2	92.3 21	.375 17		
2440.6 1	963.2 1		.889 45	380^{+625}_{-140}	355^{+415}_{-125}
2440.7 1	336.4 2	2.7 2		>595	
	920.3 1	4.0 3	<.037		
	1077.5 1	93.3 21	.055 40		
2458.4 1	146.1 2	5.9 3			
	203.0 1	94.1 30			
2479.2 1	1001.8 1	43.5 34	.515 30	49^{+6}_{-5}	
	1218.0 2	40.2 14	.489 47		
	2479.3 2	15.9 10	.372 56		
2525.1 1	287.8 1	12.8 9		160^{+25}_{-6}	
	1059.7 2	54.4 15	.320 49		

E_x^* (keV)	E_γ (keV)	Branching Ratio (%)	F(τ)	τ (fs) $(\tau_d = 0)$	$(\tau_d = \infty)$
943.3 1	943.3 1		<.036	>1150	
1363.3 1	1363.3 1		.070 19	260^{+180}_{-60}	180^{+65}_{-40}
1477.4 3	314.3 2	.9 1		>550	>300
	1477.4 1	99.1 20	<.016		
1492.5 1	1492.5 1		.366 20	32^{+3}_{-4}	
1520.5 1	1520.5 1		<.033	>930	>770
1695.1 1	202.9 1	11.8 5		80^{+15}_{-10}	
	331.9 1	6.8 7			
	1695.2 2	81.2 33	.201 17		
2142.1 1	778.8 1	13.6 2		175^{+110}_{-35}	
	2142.1 1	86.4 35	.184 61		
2162.1 1	684.7 1		<.030	>800	>200
2181.0 3	2181.0 3		.465 88	55^{+21}_{-15}	
2242.4 1	769.9 1	97.8 20	.071 23	380^{+210}_{-105}	215^{+105}_{-50}
	884.0 1	2.2 2			
2304.4 1	827.0 1		.053 16	420^{+190}_{-100}	460^{+180}_{-102}
2356.9 1	815.6 1	49.9 35	.094 16	665^{+285}_{-120}	
	893.6 1	33.2 13			

Table VI. Summary of results of Doppler-shift attenuation measurements of ^{93}Mo via the ^{93}Nb(p,nγ) reaction at E_p = 4.4 MeV.

E_x^* (keV)	E_γ (keV)	Branching Ratio (%)	F(τ)	τ (fs) $(\tau_d = 0)$	$(\tau_d = \infty)$
	1121.9 2	12.0 5			
	2535.0 2	20.0 8	.268 18		
2573.1 2	122.9 2	77.9 40		>260	
	440.9 1	22.1 15	<.133		
2642.0 1	212.1 1	29.0 15		630^{+2130}_{-150}	
	479.9 1	71.0 36	.075 59		
2644.5 2	2644.5 2		.238 77	130^{+80}_{-40}	
2668.2 1	670.9 1	26.9 10	<.122	>425	
	904.0 1	73.1 25	.039 54		
2670.1 4	2670.1 4		.564 80	32^{+12}_{-8}	
2698.0 3	2698.0 3		.433 133	54^{+40}_{-21}	
2719.5 2	1026.2 2	24.1 20		64^{+12}_{-8}	
	2719.5 2	75.9 52	.393 37		
2730.8 2	1035.6 2	15.9 15		165^{+30}_{-35}	
	2730.8 2	84.1 44	.195 27		
2742.5 10	2742.5 10		.362 85	205^{+245}_{-73}	
2755.5 1	451.1 1	87.7 28	<.069	>780	
	1778.1 1	12.3 7			
2769.2 1	1406.2 1	40.8 27		54^{+7}_{-6}	
	2769.0 1	59.2 32	.629 79		

E_x^* (keV)	E_γ (keV)	Branching Ratio (%)	F(τ)	τ (fs) $(\tau_d = 0)$	$(\tau_d = \infty)$
2810.5 1	337.2 1	60.7 16			
	369.8 1	39.3 40			
2821.5 1	1363.9 1	49.5 21	.326 27	83^{+14}_{-15}	
	1456.1 2	50.5 18			
2831.3 1	433.2 3	22.3 12		370^{+240}_{-50}	
	1136.2 2	77.7 83	.249 117		
2832.4 1	1312.2 1	61.5 32			
	1355.8 4	38.5 48			
2835.8 1	391.0 1	56.3 23		200^{+210}_{-70}	
	402.7 1	26.2 16			
	529.4 1	17.5 16	.160 87		
2834.7 2	1471.5 2				
2840.3 1	1365.2 1	50.8 37	.218 55	145^{+33}_{-25}	
	2840.3 2	46.2 16			
2858.9 1	495.8 1		.183 165	180^{+2020}_{-90}	
2862.1 4	900.5 6	95.5 102			
	2861.1 6	4.5 6			
2902.3 1	1381.7 2	35.5 78	.396 62	58^{+10}_{-5}	
	2494.9 2	13.6 13			
	1530.3 1	46.9 39	.430 28		

Table VI. (con't)

E^* (keV)	E_γ (keV)	Branching Ratio (%)	F(τ)	τ (fs) $(\tau_u \to 0)$	τ (fs) $(\tau_u \to \infty)$
	2903.5 5	4.3 6			
2915.7 1	247.5 2	14.2 12		260^{+190}_{-70}	
	668.3 1	46.8 33	.128 60		
	753.6 1	32.5 16	.134 87		
	1438.3 3	6.4 12			
2974.0 2	1454.1 4	27.1 16		185^{+55}_{-35}	
	1611.1 3	7.8 13			
	2974.0 2	65.1 22	.175 35		
3024.3 5	1547.3 5	36.9 49			
	1661.9 3	47.4 44			
	3024.3 5	15.7 22			
3048.2 1	607.6 1		<.428	>55	
3069.0 1	427.0 1	67.8 73	<.177	>180	
	1576.9 4	32.2 80			

gamma ray has the strongest angular correlation of any others observed in this reaction. The spin of this level is believed to be $17/2^+$. The lifetime, as determined by (^{7}Li, xnγ) work [18] is ∿5 nsec. We propose to measure this lifetime using the ^{93}Nb(p,nγ) reaction via the recoil distance technique. A plunger apparatus for recoil distance measurements is presently being developed for use with nuclear reactions (see Ref. 19 for details). We anticipate several more high spin states in ^{93}Mo will be populated via the ^{91}Zr(α,2nγ)^{93}Mo reaction which we are also investigating. The plunger apparatus is expected to be appropriate for measuring the lifetimes of these levels also. A program to compute the centroidshift and line shape as a function of recoil distance is being developed since the shift will be less than 1 channel in the case of the (p,nγ) reaction.

(L. L. Rutledge, E. S. Macias and D. G. Sarantites)

C. Spectroscopy and Reaction Mechanism Studies via the ^{91}Zr(α,2nγ) Reaction

Many of the lifetimes of the low-lying levels in ^{93}Mo have been determined by the Doppler-shift attenuation method using the ^{93}Nb(p,nγ) reaction at a bombarding energy of 4.4 MeV. The lifetimes of the levels also observed in the ^{91}Zr(α,2nγ) reaction will be used to study the lifetimes of the continuum cascade as a function of excitation energy and bombarding energy. If the systematics of the continuum cascade can thus be determined, it will be possible to obtain lifetimes for the new high spin levels populated via the ^{91}Zr(α,2nγ) reaction.

---

18. D.B. Fossan, private communication (1974).

19. D.G. Sarantites, USAEC Technical Progress Report COO-1530-43 (1974).

Excitation functions for the population of levels via the $^{91}Zr(\alpha,2n\gamma)$ reaction were measured. Singles γ-ray spectra were observed at an emission angle of 55° at alpha particle bombarding energies of 17, 19, 21, 24, 27, and 30 MeV. Gamma-ray energies up to 2300 keV were observed. The beam current from the isolated chamber and Faraday cup assembly was integrated to provide an accurate measurement of the beam placed on target. A strong permanent magnet placed at the entrance of the scattering chamber prevented any electrons from entering the chamber. A monitor detector at a 25° scattering angle was used to detect the elastically scattered alpha particles. The absolute cross-section of the stronger gamma rays were measured 4 times with 15 minute bombarding intervals. The stability of the beam was checked by comparing the observed elastic scattering cross-sections. The cross-sections of the weaker gamma rays were determined by comparing their peak yields to those of the previously determined gamma rays. In this case, a bombarding interval of 1 hour was used. The excitation functions provide information about the spin and parity of the levels populated, the threshold of a level, and also help to distinguish between competing reactions.

In order to provide further information about the spin and parity of the levels populated, gamma-ray angular distributions were measured at an alpha particle bombarding energy of 30 MeV. Anti-Compton singles spectra were observed at angles of 25°, 35°, 47°, 65°, 75°, and 90° relative to the beam direction. These data are being analyzed in terms of a phenominological model of the reaction mechanism in which the distribution of magnetic substates is assumed to be gaussian following the nuclear reaction. The width of the gaussian is adjusted to fit the data. It is hoped that this technique for calculating the alignment will also enable us to determine the multipol mixing ratios from these data. A computer program for this type of analysis is being developed.

Anti-Compton gamma-ray spectra were measured at emission angles of 25°, 47°, 65°, 75°, and 90° in order to determine the lifetimes of levels populated via the $^{91}Zr(\alpha,2n\gamma)^{93}Mo$ reaction via the Doppler-shift attenuation method. The experiment was performed at bombarding energies of 21, 24, 27, and 30 MeV. Gamma-ray energies were observed up to 2300 keV. Internal energy standards were counted simultaneously with the reaction gamma-rays to provide an accurate measurement of the photopeak centroid energies. A computer program to compute to the cone of recoiling ^{93}Mo nuclei following the $(\alpha,2n)$ reaction is being developed. This information combined with cascade feeding systematics discussed above and the bound state feeding determined by γ-γ coincidence experiments will allow lifetime measurements of the levels for $\tau \leq 2$ psec using the LSS[20,21] stopping power of the recoiling ions.

A γ-γ coincidence experiment will also be performed at an alpha particle bombarding energy of 30 MeV. These data are needed to construct the complete decay scheme of levels populated in the $^{91}Zr(\alpha,2n\gamma)$ reactions.

(L. L. Rutledge, E. S. Macias and D. G. Sarantites)

D. G-Factor Measurements

Doppler-shift attenuation measurements in this lab[19] have indicated that the 7^+ level at 2282 keV in ^{56}Co and the 6^+ level at 3389 keV in ^{56}Fe have lifetimes >2 psec. The levels are populated via the $^{54}Fe(\alpha,pn)$ and $(\alpha,2p)$ reaction respectively at an alpha particle bombarding energy of 24 MeV. These levels are good candidates for magnetic moment measurements using the implantation perturbed angular correlation technique. However it

---

20. L. Lindhard, M. Scharff and H.E. Schiott, K. Dan. Vidensk. Selsk. Mat.-Fys. Medd. 33, (14) (1963).

21. A.E. Blaugrund, Nucl. Phys. 88, 501 (1966).

will be necessary to first measure the lifetimes of these levels using the plunger apparatus described earlier. The magnet and scattering chambers for the magnetic moment measurements have been designed and are being built.

(L. L. Rutledge, D. G. Sarantites and E. S. Macias)

III. Instrument Development

A. On-Line Determination of Transport Time of a Helium-Jet System

This work has been completed and accepted for publication in Nuclear Instruments and Methods. A preprint of this work accompanies this report. The abstract is given below:

> A rapid and accurate method for determining the recoil transport time of a helium-jet system by measuring the output activity ratio of two nuclides produced in a single charged particle bombardment with known cross-section is given. The minimum transport time of the Washington University helium-jet system (149 ± 29) ms. was determined using this method with the 0.21 and 78 s isomeric states of ^{109}In. For a 25 MeV alpha-particle bombardment of natural silver the ^{109}In cross-section ratio was found to be $\sigma_{0.21s}/\sigma_{78s} = 0.41 \pm 0.40$

(E. S. Macias, R. E. Head, H.-C. Hseuh, and M. R. Zalutsky)

B. Improvement of the Washington University Helium-Jet/Tape Transport System

The Washington University helium-jet/tape transport system has been improved during the past year in several ways. The original capstan drive motor (Superior Electric Slo-Syn model TS-50) was replaced with a new high speed stepping motor (Superior Electric Slo-Syn model M112-FJ12). A new translator was also built for this motor. This system has a torque of 400 oz-in at a typical driving speed of 400 msec per tape movement. This is a factor of 10 improvement in torque over the old motor.

The tape drive was also modified for coincidence experiments to allow the placement of two detectors both within 2 cm of the source.

(E. S. Macias, L. Djordjevic, R. E. Head, H.-S. Hseuh and M. R. Zalutsky)

C. A Simple Fast Sweeping System for Extracted Cyclotron Beams

This work has been completed and published in Nuclear Instruments and Methods 119, 213 (1974). A reprint of this article is appended to this report. The abstract is given below:

A simple system for sweeping an extracted cyclotron beam on and off an adjustable aperture at various repetition rates and duty cycles is described. This system permits lifetime measurements of delayed γ-rays to be made over a range of 0.5 to 5000 μs. The application of this system for the study of the 3.29 and 159 μs isomeric states in ^{115}Sn populated by the (p,nγ) reaction at 8.0 MeV is described.

(J. T. Hood, R. A. Goldworm, E. S. Macias and D. G. Sarantites)

D. Development of an Electron Gun for Thin Target Fabrication

The plunger apparatus for recoil distance measurements requires targets of ∿50 μgm/cm^2 thickness. In order to prepare thin plunger targets such as niobium (mp.p = 2468° C) and zirconium (m.p. = 1852° C) a Varian 2-KW single crucible electron gun evaporation source has been obtained. This source utilizes permanant-magnet focusing, and can achieve target temperatures to 3500° C. Safety interlocks on the cooling water and filament supply have been installed. High vacuum-high voltage interlocks are presently being installed. The accelerating voltage is 4000 volts. We have achieved an emission current of 350 ma for 2 min at the required accelerating voltage. An emission current of 500 ma must be sustained in order to evaporate the niobium or zirconium metal

(R. E. Head, J. Hood, L. L. Rutledge, and E. S. Macias)

E. Application of the Beta Attenuation Technique for the Determination of Cyclotron Target Thickness

The use of thin targets in recoil distance measurements necessitates an accurate method for accurately determining target thicknesses as thin as ~50 $\mu gm/cm^2$. The attenuation of electrons emitted from a low energy beta source has been previously suggested for this purpose but is not widely used.[22-24] Our experience with the beta attenuation technique for atmospheric aerosol mass measurement (see Part IV of the report) indicated that a simple inexpensive beta attenuation device could be constructed for determining thin cyclotron target thickness. We have built a prototype beta attenuation scanner employing a ^{14}C beta source and silicon surface barrier detector coupled to fast low-noise nuclear electronics. We are now testing this device with targets made of various elements.

(E. S. Macias, R. Goldworm and L. L. Rutledge)

F. Calibrations of Ge(Li) and Si(Li) Detectors

Recent advances in the spectroscopy of x rays and low energy gamma rays have been in part due to the increased quality of commercially available semiconductor spectrometers. Use of these detectors requires careful calibration of absolute efficiency and silicon escape peak efficiency. These calibrations are described below.

1. X-ray detector efficiency determinations

The efficiency calibration of a detector for energies less than 100 keV requires standards for which the relative intensity of both γ rays and x rays are well known. This necessitates accurate values for fluorescence

---

22. J.H. Peterson and J.R. Downing, J. Opt. Soc. Am. 41, 862 (1951).

23. B.D. Pate and L. Yaffe, Can. J. Chem. 33, 15 (1955).

24. O.U. Anders and W.W. Meinke, Rev. Sci. Inst. 27, 416 (1956).

yields, conversion coefficients, and electron capture probabilites. The decay characteristics of several low-energy photon standards have been recently reported.[25-27] Of these suggested sources, ^{241}Am, ^{137}Cs, ^{109}Cs, and ^{57}Co were chosen for use as efficiency standards. A ^{182}Ta source was also used as a relative standard for the efficiency calibration of the 80-220 keV region.[28] The decay data for the calibration standards used in these measurements are given in Table VII.

Each source was counted in a fixed geometry using a lucite source holder fastened to the end of the detector. The source-to-crystal distances were 1.6 cm and 2.6 cm for the Si(Li) and Ge(Li) efficiency determintaions, respectively. Counting rates were less than 1000 counts/sec for all measurements to minimize pulse pileup in the amplifier. This was particularly important for the calibration of the Si(Li) detector because an amplifier shaping time of 6 μsec was necessary for optimum energy resolution.

Absolute photopeak efficiences were calculated by dividing the net photopeak counting rate by the absolute photopeak intensity. An absolute photopeak efficiency curve was then constructed for each detector and the data from the relative standards were fit to these curves. The resultant efficiency curves for the Si(Li) and the Ge(Li) detector are shown in Fig. 13. The major sources of error in these measurements are the uncertainties in the relative photon intensities which are given in Table VII and the uncertainties in the counting statistics of 0.5-3.0%.

---

25. R.J. Gehrke and R.A. Lokken, Nuc. Inst. and Methods 97, 219 (1971).

26. J.L. Campbell and L.A. McNelles, Nucl. Inst. and Methods 101, 153 (1972).

27. J.L. Campbell, P. O'Brien, and L.A. McNelles, Nucl. Inst. and Methods 92, 269 (1973).

28. D.H. White, R.E. Birket, and T. Thomson, Nucl. Inst. and Methods 77 261 (1970).

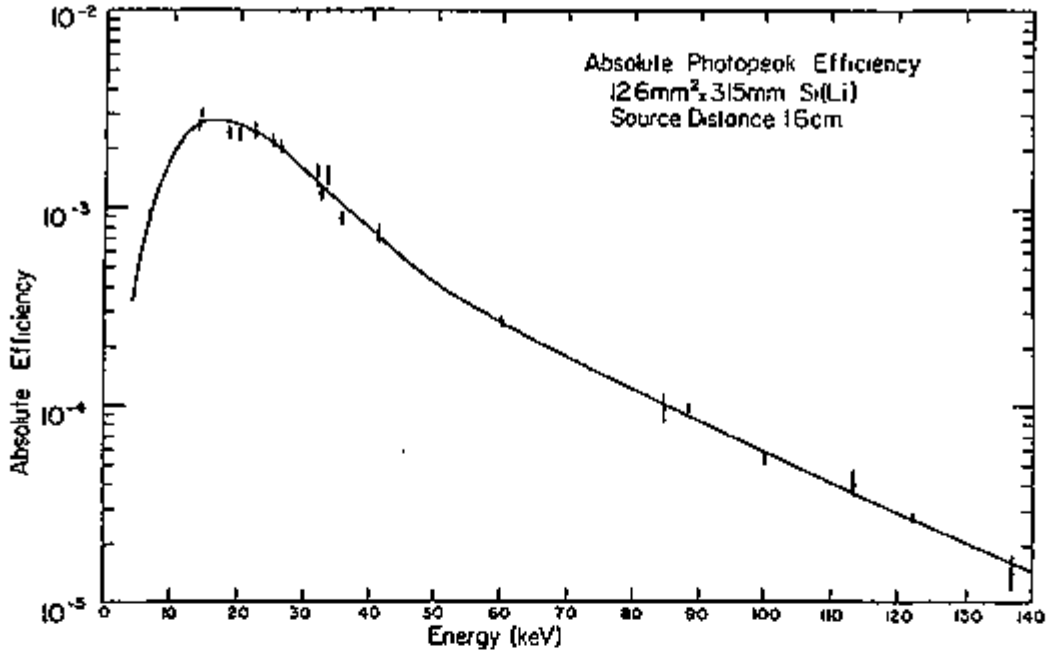

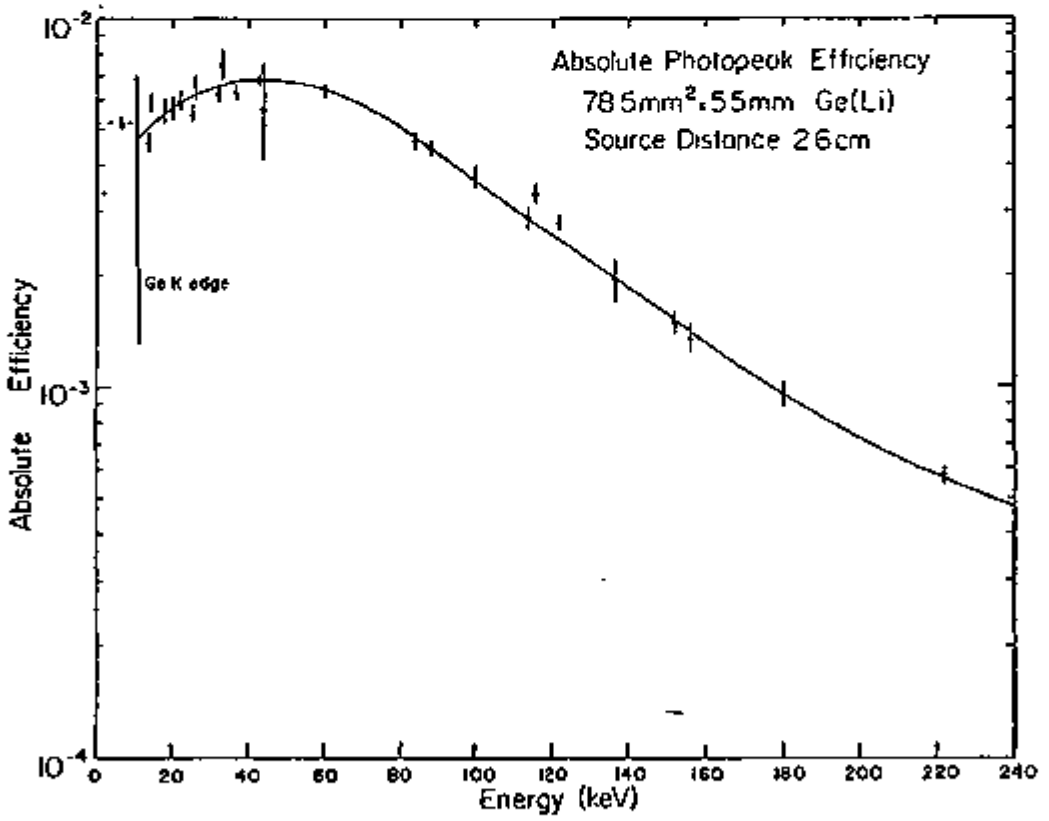

Figure 13. Absolute photopeak efficiency curves for our Ge(Li) and Si(Li) x-ray spectrometers.

Table VII. Intensity data used for the determination of x-ray detector efficiencies.

Source	Half life	E_γ (keV)	I_γ	reference
^{241}Am	432.9 y	13.9 (Lα)	35.1 ± 2.5	25
		17.8 (Lβ)	53.2 ± 3.8	
		20.1 (Lγ)	13.3 ± 1.0	
		26.3	6.2 ± 0.5	
		33.2	0.29 ± 0.03	
		43.5	0.16 ± 0.05	
		59.5	(100)	
^{137}Cs	30.5 y	32.1 (Kα)	6.6 ± 1.6	26
		36.6 (Kβ)	1.6 ± 0.4	
^{57}Co	272 d	6.5 (K)	54.7 ± 1.3	27
		14.4	9.4 ± 0.2	
		122.0	84.5 ± 1.5	
		136.3	11.9 ± 1.3	
^{109}Cd	453 d	22.1 (Kα)	21.61 ± 0.43	26
		25.0 (Kβ)	4.59 ± 0.13	
		88.0	(100)	
^{182}Ta	115 d	42.7	0.70 ± 0.04	28
		84.1	7.64 ± 0.37	
		100.1	40.7 ± 1.5	
		113.7	5.53 ± 0.30	
		116.4	1.28 ± 0.08	
		152.4	21.0 ± 0.8	
		156.4	8.1 ± 0.4	
		179.4	9.44 ± 0.40	
		198.4	9.37 ± 0.35	
		222.1	22.7 ± 0.9	

2. Silicon x-ray escape peak correction

If the x rays emitted by the silicon atoms in the Si(Li) crystal escape from the crystal, the energy deposited in the detector will be

$$E'_x = E_x - E(B)_{Si} \quad (1)$$

Here, E_x is the energy of the incoming x ray, E'_x is the energy deposited in the crystal, and $E(B)_{Si}$ is the binding energy of silicon, 1.74 keV.

A correction for the presence of a silicon x-ray escape peak under a lower energy photopeak will be necessary when

$$E_x = (1.74 \pm \text{FWTM}) \text{ keV} \quad (2)$$

where E_x is the energy difference between two x rays and FWTM is the full width at tenth maximum of the Si(Li) detector at energy E_x.

The silicon x-ray escape peak efficiency was determined by measuring the ratio of counts in the escape peak relative to the number of counts in the photopeak detected in the Si(Li) crystal for the low energy photons (<14 keV) from ^{57}Co and ^{54}Mn sources. These data were then fit to a curve dervied from Axel's formula[29] for the x-ray escape peak probability of a similar dimensioned Si(Li) detector.[30]

G. New Lithium Drifted Germanium Detector

A new 11.7% true coaxial Ge(Li) detector was purchased during the past year. This detector has an energy resolution of $\leq$2.2 keV at 1332 keV.

---

29. P. Axel, BNL 271 (T-44) (1953).

30. R.E. Wood, P. Venugopala Rao, O.H. Puckett and J.M. Palms, Nucl. Inst. and Methods 94, 245 (1971).

IV. Environmental Studies: High Resolution On-Line Aerosol Mass Measurement by the Beta Attenuation Technique

The following is a brief description of work carried out under the sponsorship of the United States Environmental Protection Agency. This material was presented at the Second International Conference on Nuclear Methods in Environmental Research, Columbia, Missouri (1974) a conference sponsored jointly by the USAEC and several other agencies.

Atmospheric aerosols (particulates) are receiving increasing attention of air pollution control agencies. The main reason is that aerosols are associated with many of the harmful or annoying air pollution effects: visibility degradation, health associated effects, soiling of property, etc. In the past particulates were generally considered as a single pollutant. The characteristic parameter that was used to quantify the aerosol concentration was the total mass concentration ($\mu gm/m^3$) measured by the high-volume air filter sampler.

Recently it has been recognized that atmospheric aerosols need to be characterized by several parameters in addition to the total mass concentration. This is because particulates are distributed with respect to size and chemical composition and that each of the major effects are associated with a specific size range and chemical composition.

However, this apparently complex situation may be simplified as shown recently in studies on the physico-chemical properties of atmospheric aerosols.[31-33] This work revealed that in general the atmospheric aerosol

31. K.T. Whitby, R.B. Husar, and B.Y.H. Liu, J. Colloid Interface Sci. 39, 177 (1972).

32. D.L. Lundgren, H.J. Paulus, Presented at the 167th American Chemical Society Meeting, Division of Environmental Chemistry, Los Angeles (197

33. J.L. Durham, W.E. Wilson, K. Willeke, and K.T. Whitby, Presented at the 167th American Chemical Society Meeting, Division of Environmental Chemistry, Los Angeles (1974)

mass is distributed bimodally; the lower mass, or fine particle mode being in the size range between 0.1 and 1.0 μm, while the upper, or coarse particle mode was found to be over 5 μm. The saddle point between the two mass (or volume) modes is between 0.8 and 3.0 μm. It is anticipated that within the next few years these findings will be recognized by establishing new standards requiring the determination of aerosol mass and composition as a function of particle size. Independent determination of the mass concentration of only two size fractions, divided at about 1 to 3 μm will probably be adequate for monitoring purposes.

The high volume filter technique and other gravimetric weighing methods currently in use for atmospheric monitoring are inadequate for future monitoring purposes. Slow time response and tedeous manual operation are the principal disadvantages of these methods.

We have developed a two stage on-line mass monitor with aerosol size separator (TWOMASS) employing the beta attenuation technique for high resolution monitoring of atmospheric aerosols. This instrument independently analyzes the mass concentration of two particle size fractions. Coarse particles are inertially separated by impaction on mylar film coated with a silicon adhesive. The fine particle fraction is collected on a high efficiency glass-fiber filter. Carbon-14 is used as a source of beta particles which are detected by a solid-state silicon surface-barrier detector coupled to fast low-noise nuclear electronics. The output of this system is sent to a high speed counter interfaced to a programmable calculator which controls TWOMASS, calculates mass concentration of each size fraction, plots, prints and stores the data on tape. The instrument has been gravimetrically calibrated using laboratory aerosols. It has subsequently been

field tested by sampling atmospheric aerosol over a one week period which indicated that it is capable of ambient air monitoring with a time response on the order of ten minutes.

Level of Effort

The principal investigator has spent 50% of his time during three summer months and 25% of his time during the six academic months on work supported by this contract. It is anticipated that the principal investigator will spend 25% of his time on this project for the remaining three months of the contract year.

Personnel

Principal Investigator

Edward S. Macias, Assistant Professor of Chemistry

Research Associate

Loyd L. Rutledge

Graduate Research Assistants

Hsiao-Chaun Hseuh
Michael R. Zalutsky

Undergraduate Research Assistants

Eric Scott Jenson
David Alan Simon
Luis Enrique Zapata

Electronics Technician

Lazar Djordjevic

Other Involved in this Work but not Supported under this Contract

D.G. Sarantites, Associate Professor of Chemistry
R.B. Husar, Associate Professor of Mechanical Engineering
R.A. Meyer, Lawrence Livermore Laboratory
J. Hood, Cyclotron Director
R. E. Head, Cyclotron Engineer
R. Goldworm, Graduate Student